J. Electrochem. Sci. Eng. **13(6)** (2023) 971-980; http://dx.doi.org/10.5599/jese.1899

Open Access : : ISSN 1847-9286
https://pub.iapchem.org/ojs/index.php/JESE

Original scientific paper

Influence of polarization curve slope on the accuracy of local copper electrodeposition from sulphate electrolyte

Georgii Vasyliev✉, Viktoria Vorobyova, Dmytro Uschapovskiy, Mykhailo Kotyk and Olga Linucheva

National Technical University of Ukraine "Igor Sikorsky Kyiv Polytechnic Institute", 37, Prospect Peremohy, Kyiv-56, 03056, Ukraine

Corresponding authors: ✉g.vasyliev@kpi.ua; Tel.: +38-096-924-9888; Fax: +38-044-204-9773

Received: March 22, 2023; Accepted: June 24, 2023; Published: June 27, 2023

Abstract

Local electrochemical deposition is an emerging technique, used in the field of additive manufacturing. The advantage of electrochemical additive manufacturing lies in the utilization of room temperature electrolyte and permits to manufacture microscale objects with high precision. The increase in deposition current increases the deposition area, so measures are to be taken to focus the electric field. This work describes the influence of polarization curve slope on the accuracy of local deposition, both experimentally and by computer modelling. The copper was deposited using rotating anode on the surface of stainless steel from sulphate electrolyte. The influence of electrolyte composition on the accuracy of deposition was investigated. The profile of deposited parts was analyzed by profilometry and microscopy. The increased amount of sulfuric acid and presence of the additive in the electrolyte was shown to increase the accuracy of deposition by changing the slope of cathodic polarization curve from 320 to 1100 mA $V^{-1}cm^{-2}$.

Keywords

Additive manufacturing; 3D printing; copper electroplating; throwing power, profilometry

Introduction

Additive manufacturing (AM) or 3D-printing is a manufacturing technique, rapidly developing in recent years. AM utilizes a bottom-up approach, when the material is added layer by layer, in contrast to traditional manufacturing techniques, where the needed part is produced from blank though removing the excess material. The cost of 3D-printed parts decreases, with the increase of part complexity, due to lower consumption of material, despite subtractive production, where the more complex part is, the more operations is required for its production. Thus, the research in the field of AM is of extreme importance [1].

Metal AM remains one of the most demandable techniques, because metals remain on the first positions of the world most used materials. The existing metal AM techniques require application

of high energy devices for local metal melting: selective laser melting (SLM) and electron beam melting (EBM) [2-5], and the precision of AM is limited to the size of a metal powder (for laser or electron beam sintering). Unlike them, electrochemical additive manufacturing (ECAM) enables AM production at room temperature by using the metal electrodeposition principles [6-7].

Electrochemical deposition enables the use of the smallest species of a material – ions. Other techniques use metal powders or wires, that are bigger sizes. Thus, the main investigation direction is electrochemical additive manufacturing of micron and submicron scale objects. The application of fluidic force microscope (FluidFM) permits the production of pillars, needles, helix, connectors, and other objects of only few micrometers in size [8-12]. The technique is extremely precise; however, the deposition rate is slow.

A faster approach for bigger objects is a meniscus confined deposition [13-18]. Here the deposition is located in the small volume of electrolyte solution between the capillary and substate. The anode is placed inside the capillary and the substrate is polarized cathodically. This technique permits to print flat objects; however, they can be produced from different metals, that are deposited layer by layer. The deposition rate is faster than FluidFM technique, because the volume of electrolyte is larger, however, the growth rate is determined with the diffusion rate of metal ions in meniscus.

Even faster deposition rates can be achieved using electrodeposition from a large volume of electrolyte [14-26]. High deposition rate requires high concentration of metal ions, that makes an electrolyte conductive and electric field distributes easily around the anode. To localize the deposition region, masks are applied on the substate [27], or the size of the anode is miniaturized [28]. Typical objects are printed by sequential deposition of the metal under anode until deposited layer touches the anode. After this, the anode is moved to another position or upwards and the process repeats. In this condition, the deposition is also limited by the diffusion rate of metal ions, but their concentration is much higher than in meniscus deposition. To achieve higher deposition rates the pulsed current is applied instead of constant.

The aim of this work was to test the influence of copper plating electrolyte composition on the accuracy of local deposition in conditions of working electrode rotation.

Experimental

Local electrochemical deposition

The electrodeposition process was organized in the electrochemical cell. The stainless-steel plate AISI 321 was placed on the bottom of the plastic vessel and was connected to the negative pole of current source. The stainless-steel was chosen to ensure separation of the printed part from the base after deposition. The working electrode was rotated with an electric motor, the rotation speed was 1 s^{-1}. The working electrode was a cylinder-shaped platinum foil, connected to the positive pole of current source. The design of the laboratory set-up is given in Figure 1.

The stainless-steel substrate was polished with SiC emery paper, degreased, and placed on the bottom of the vessel. The 1 L of electrolyte solution was poured into the vessel, the level of electrolyte was 20 mm above the substrate. The composition of the electrolyte is given in Table 1. The anode was placed 5 mm above the substrate and started to rotate. The current was applied with a density of 40-50 mA cm^{-2}, for the 60-460 min.

After the deposition, the current was turned off, the solution was drained from the vessel. The deposited part in the form of the ring was cleaned with distilled water, removed from substrate, and investigated. The experimental conditions are provided in Table 2. Expected thickness was calculated by COMSOL software, based on Faraday's law.

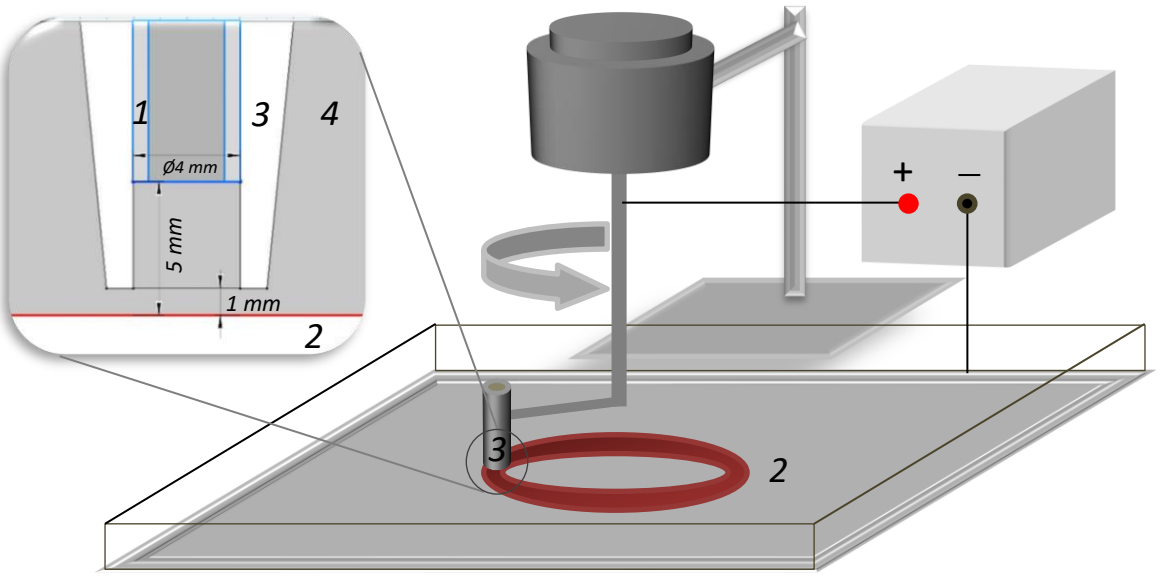

Figure 1. *The scheme of laboratory set-up: 1 - platinum foil (anode); 2 - stainless steel base (cathode); 3 - polypropylene capillary; 4 - electrolyte*

Table 1. *Electrolyte composition*

Component	Content, g L^{-1}	
	Electrolyte 1	Electrolyte 2
$CuSO_4 \cdot 5H_2O$	200	200
H_2SO_4	10	75
KCl	1	0.3
$Fe_2(SO_4)_3$	10	-
Gelatine	0.05	-
Additive RUBIN T-200*	-	2 mL L^{-1} of RUBIN T200-A; 8 mL L^{-1} of RUBIN T200-G 2 mL L^{-1} of RUBIN T200-E [29]

**Leveling and brightness additive, KIESOW OBERFLÄCHENCHEMIE GmbH & Co. KG*

Table 2. *Experimental conditions*

Sample number	Electrolyte	*i* / mA cm^{-2}	Expected thickness, μm
1	1	11	20
2	1	20	40
3	2	40	50
4	2	50	50
5	2	40	200
6	2	50	200

Local electrochemical deposition

The geometry of printed objects was analyzed (Figure 2).

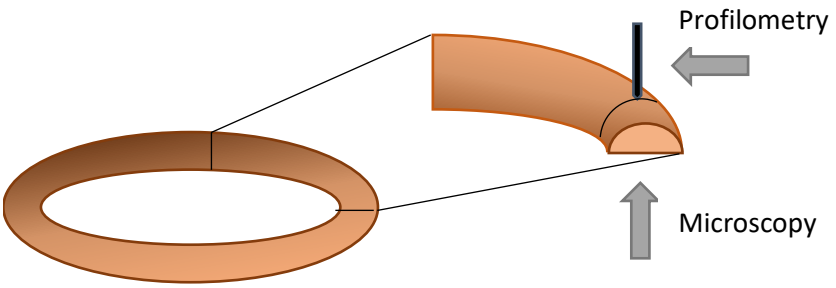

Figure 2. *The scheme of locally deposited metal characterization*

For this purpose, the profilograms of the rings were measured in 4 positions (every 90°). The profilometry results were compared to the thickness measurements on the cross-sections of the printed rings. The sections of the rings were cut, sealed with epoxy resin, polished, and prepared for optical microscopy. The cross section of the printed rings was observed using iScope IS.1053-PLMi optical microscope (Euromex Microscopen BV). The accompanying software was used to conduct linear measurement.

Results and discussion

Copper deposition is an electrochemical process of Cu^{2+} ion reduction on the surface of negatively charged substrate. The electrochemical reaction can be expressed by the following reaction:

$$Cu^{2+} + 2e^{-} = Cu \quad (1)$$

The rate of the reaction is expressed in terms of electric current that passes through the electrochemical cell and corresponds to the number of copper ions being reduced in certain time intervals. The deposited copper ions form a metal lattice. The dependence between the charge passed through the cell, and the mass of the deposited metal is expressed by the Faradays law:

$$m = MIt / zF \quad (2)$$

where m /g is the mass of deposited metal; M / g mol^{-1} is atomic mass; I / A us current; t / s is time,; z is number of electrons required for ion reduction; F / C mol^{-1} is the Faraday constant,.

The dependence between the applied voltage and the deposition rate is expressed by the current-voltage dependence or the polarization curve. The typical polarization curve for copper deposition is given in Figure 3. Two regions can be determined in the curve. The first one shows the growing current-voltage dependence and is characterized by the slope of polarization curve di/dE. The second region is a limiting current region, where deposition rate is independent of the applied potential. The limiting current, i_{lim}, can be increased in the same electrolyte by applying electrode/electrolyte movement, see curves 1 and 2.

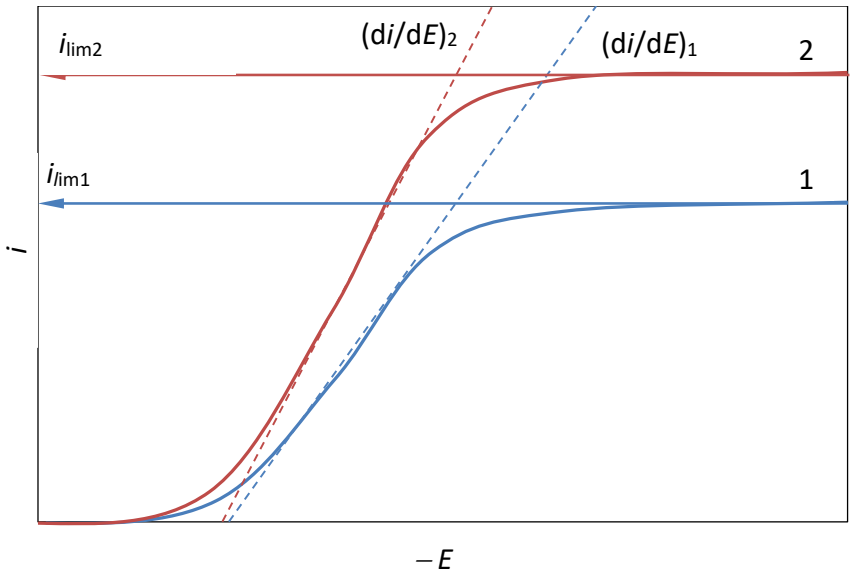

Figure 3. *Typical polarization curve for copper deposition: 1 - stationary deposition; 2 - relative movement of electrode and solution*

COMSOL MULTIPHYSICS 4.3 (https://www.comsol.com/) [30] was used for computer modeling of the secondary distribution of the current density in the space between the electrodes (the working area of the 3D printer) and on the surface of the cathode. Based on the built-in model of

"Long-term growth of copper deposits" [20], a model of the working area of the 3D printer was developed (Figure 1). The used model can be described by the following equations.

Electric field distribution in the body of the electrodes:

$$\nabla \mathbf{i} = 0, \mathbf{i} = \sigma \nabla V \quad (3)$$

Electric field distribution in the volume of the electrolyte:

$$\nabla \mathbf{i} = 0, \mathbf{i} = \kappa \nabla \varphi \quad (4)$$

On the surface of electrodes, the simplified linear dependence was used:

$$\mathbf{i}\,\mathbf{n} = b\ \eta \quad (5)$$

$$\eta = V - \varphi - E^0 \quad (6)$$

where: **i** – the current density; σ and κ – electrical conductivities of electrode material and electrolyte, respecxtively; V – cell voltage; η – overvoltage; b – constant; **n** – the normal vector, pointing out of the domain; φ – potential in the electrolyte; E^0 – equilibrium electrode potential.

The distribution of the current density in the electrolyte corresponds to the secondary one and depends both on the geometric parameters of the cell and characteristics of the electrode reaction, the polarization of the cathode and is generally described by the Wagner criterion [30,31]. It is also assumed that the electrical conductivity of the solution in the interelectrode space is constant. In particular, one of the determining parameters according to the used model [30], is the derivative of the current density by overvoltage (di/dE). This value is determined based on the polarization characteristics of the working electrodes of the used electrochemical system and corresponds to the slope of their linear sections.

The polarization curves for the two tested electrolytes are given in Figure 4. Polarization parameters and electrolyte conductivity used in the computed model are given in Table 3.

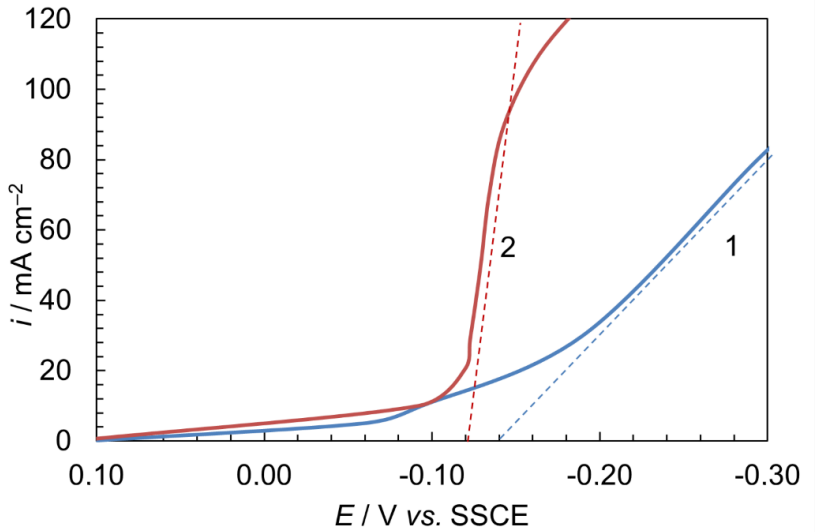

Figure 4. *The stationary cathodic polarization curves of copper deposition: 1 - Electrolyte 1; 2 - Electrolyte 2. Potentials are given* vs. *saturated silver chloride electrode (SSCE)*

Table 3. *Electrochemical parameters of the electrolyte*

Electrolyte number	σ / S cm^{-1} [32]	(di/dE) / mA V^{-1} cm^{-2}	Applied voltage, V
1	0.068	320	0.3-0.5
2	0.231	1100	0.2-0.5

The results of electrochemical manufacturing are given in Figure 5. The copper deposits obtained from Electrolyte 1 at a current density of 10-20 mA cm^{-2} were mostly fine-crystalline and had a light

color. At the same time, their thickness did not exceed 40 µm. The copper deposits obtained from electrolyte 2 at current densities of 40-50 mA cm^{-2} had a compact but coarser crystalline structure and a darker color. In particular, the formation of spherulitic deposits was observed at a deposit thickness of 200 µm, electrodeposited at a current density of 50 mA cm^{-2}. The metallic copper is deposited in the form of rings, easily detached from the stainless-steel substrate. The morphology of the deposited rings was investigated using profilometry technique. The profilometry results are given in Figure 6, along with the profile of deposited metal, calculated using the Comsol Multiphysics software. The height of the deposited copper agrees with the results of computer modelling. The modelled profile shows the typical shape of Gaussian distribution. The shape of the real deposited copper profile differs from normal distribution.

The profile of deposited copper has an uncommon shape, with the increased height at the edges. This is caused by the internal stress of copper deposits. As it can be seen from the deposited profile, this is tensile stress. The reason for tensile stress is the formation of crystal lattice defects, caused by the presence in the electrolyte of surface-active substances [33].

Due to absorption and incorporation in metal structure of surface-active substances during electrodeposition the defects of crystal lattice appear, namely vacancies. The presence of vacancies leads to the deformation of metal structure. In this case of local electrodeposition, the electrolyte contains gelatin and iron (III) sulphate, that cause vacancies incorporation in the lattice.

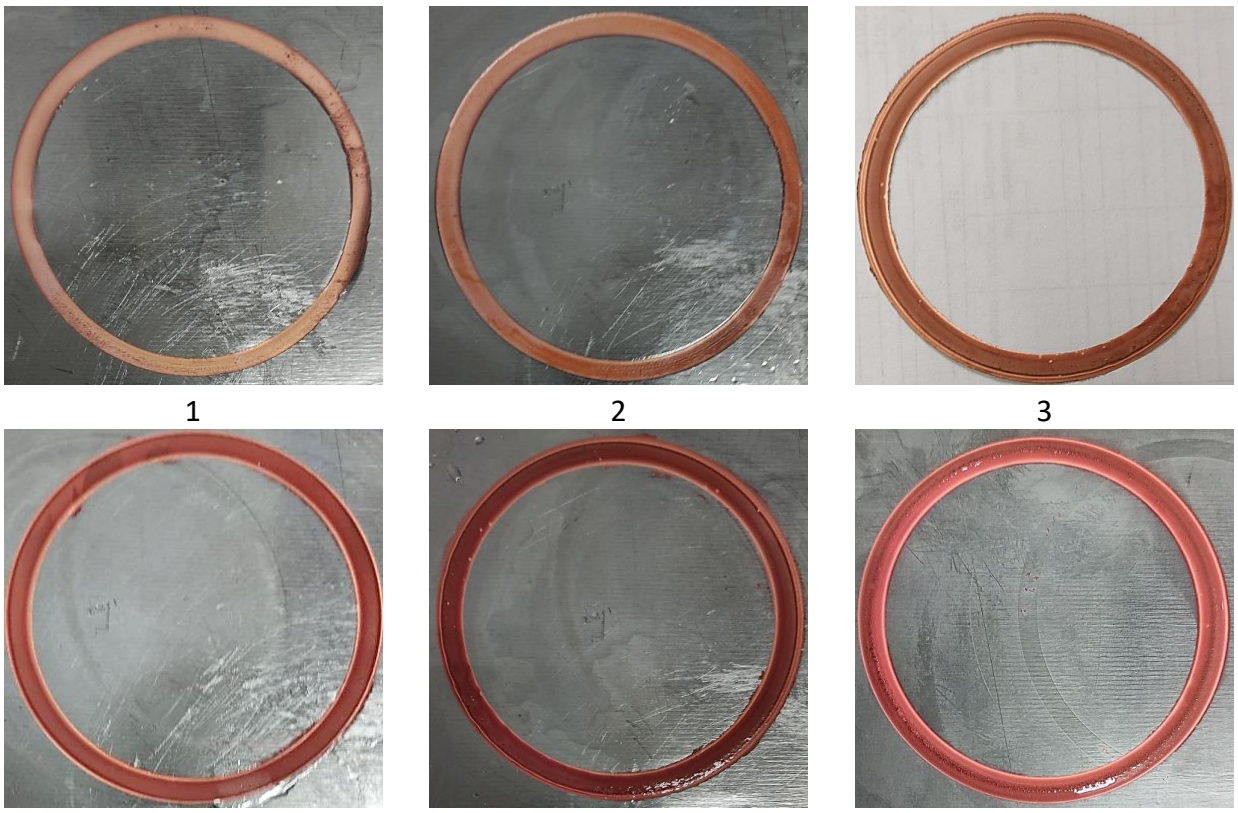

Figure 5. *Copper rings manufactured by local electrodeposition using rotating anode*

While the thickness of deposited metal agrees well with the model, the thickness distribution under the anode is different. In particular, the area of metal deposition under the anode in computer model is wider than the experimental one. The following explanation may be suggested. The COMSOL software models the deposition profile using the constant polarizability of the process. At the same time, the real polarization curve (Figure 4, curves 1, 2) has a constant slope value only in

a short potential range. Below this potential range, the slope differs, so practically no deposition may occur. That is what can be seen from Figure 6.

On the other hand, according to the theory of electrocrystallization [34] in the range of low current densities (the polarization resistance range), which is characterized by a linear current-potential dependance, metal deposition occurs in the singe crystal form. Some parts of the surface are not suitable for deposition at all. Moreover, it is worth mentioning that electrodeposition was performed on the surface of stainless steel. The base, made from metal different from the deposited one, also leads to the increase of phase overvoltage and, as a result, to the reduction of deposition rate in the low current density regions. The latter also suggests using stainless steel as a base metal for 3D electrochemical printing.

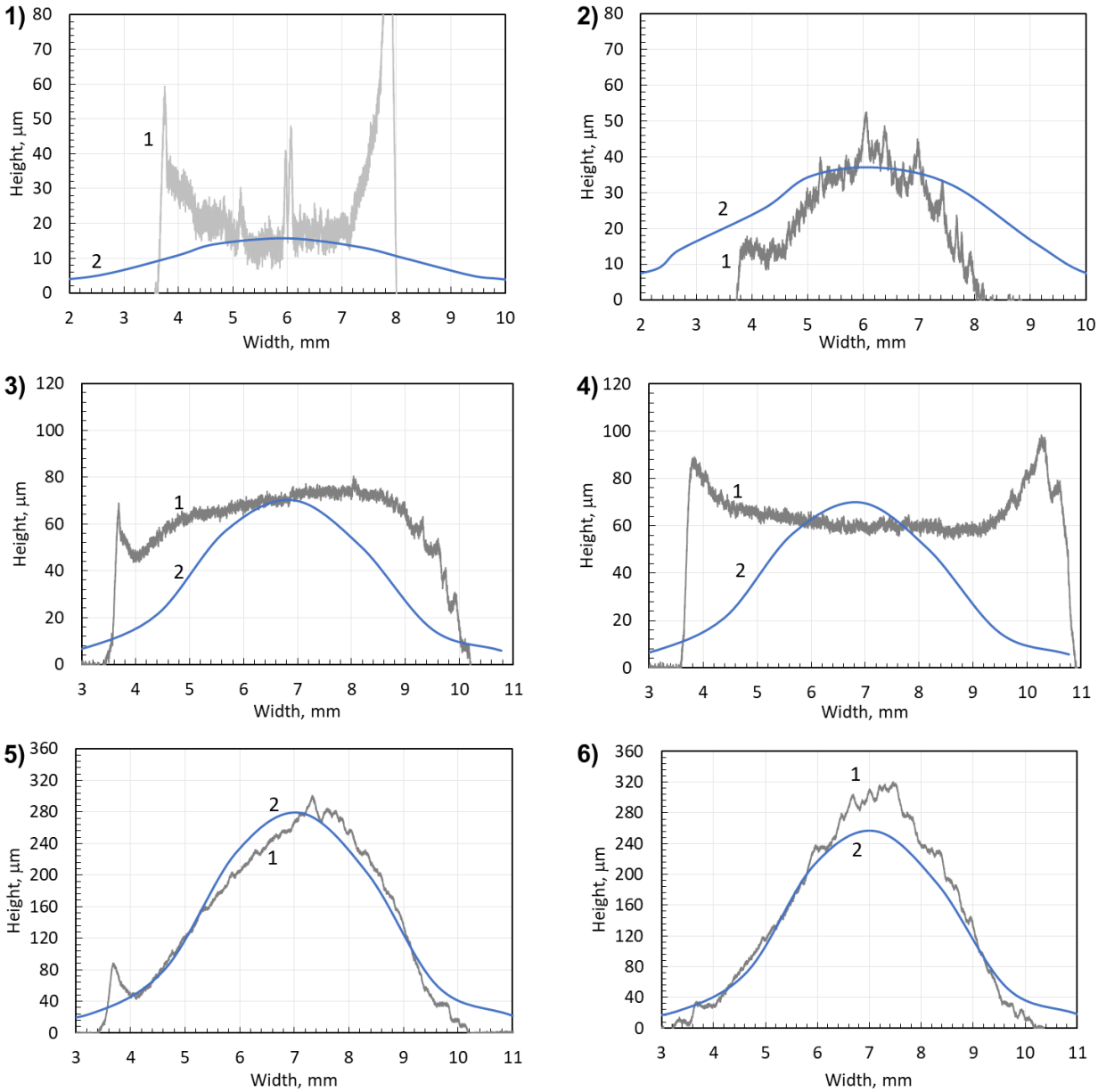

Figure 6. *The profile of deposited copper parts: 1 - averaged profilometry results; 2 - computer simulation of deposited copper*

The thickness values measured in the profilometry test agree well with the results of cross-section microscopic investigation (Figure 7). However, the microphotographs show no wrapped edges, so the thickness measurements were performed accurately. Samples 1-5 show dense metal

structure on the cross-section, but sample 6 appeared to be fractured. This was caused by the application of high current density, 50 mA/cm^2. This led to the formation of powder-like large copper crystals with low cohesion. So, current density above 40 mA/cm^2 should not be recommended when objects higher than 50 μm are electrodeposited.

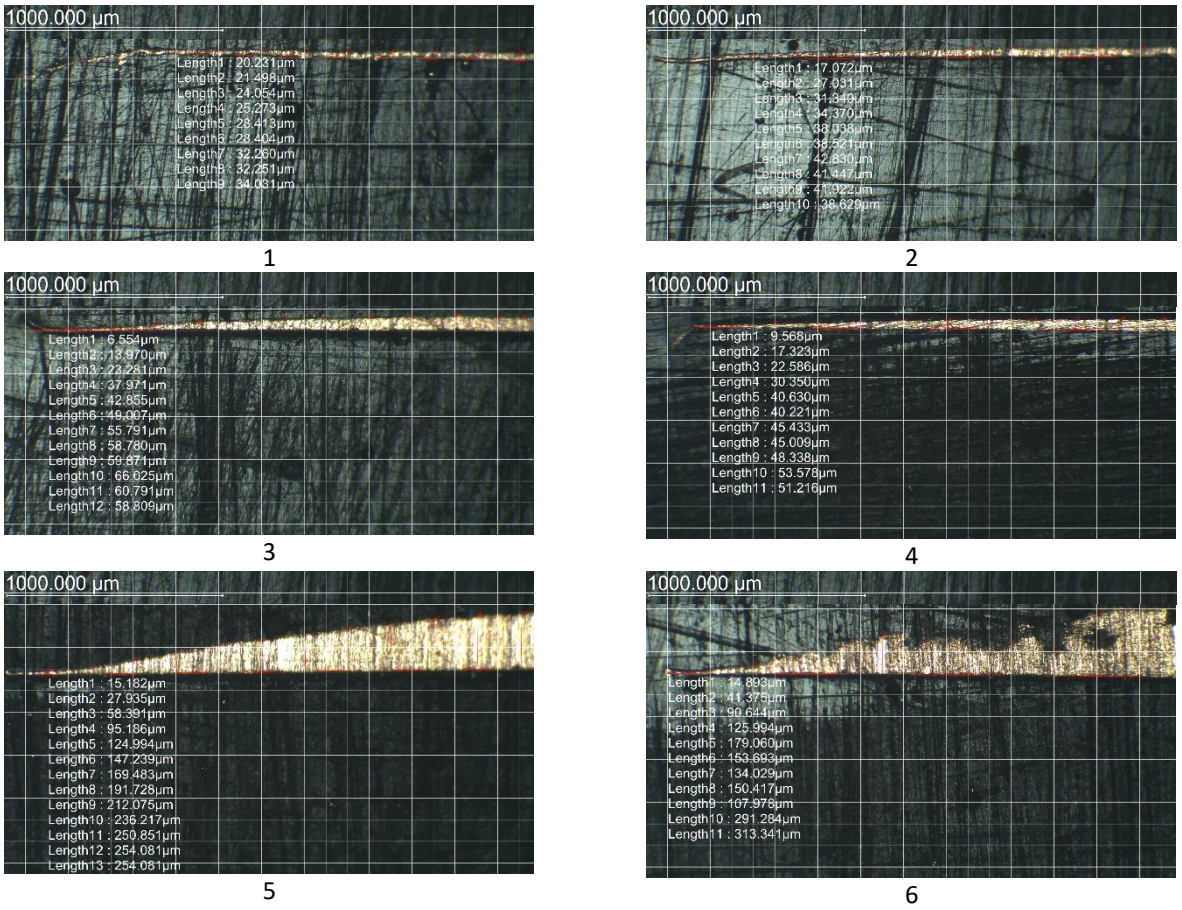

Figure 7. *Cross-section photographs of deposited copper rings*

Conclusions

1. Local electrochemical deposition makes it possible to form parts from aqueous solutions without the use of high energy.
2. It is possible to increase the accuracy of printing by choosing an electrolyte that has a narrow range of deposition potentials. When the polarizations value is below this region, no deposition occurs. In this work, the additive RUBIN T-200 efficiently prevented deposition at low potentials.
3. The differences in the deposits profile in the model and the experiment are caused by the fact that the model assumes a linear dependence of polarization in the entire range of potentials. In fact, this is true only for a certain range of potentials.

Acknowledgments: *The work was supported by the Ministry of Science and Education of Ukraine, state registration number 0122U001523, 2022.*

References

[1] I. Gibson, D. Rosen, B. Stucker, *Additive Manufacturing Technologies*, Springer, New York, USA, 2010, p. 472. https://doi.org/10.1007/978-1-4419-1120-9

[2] L. E. Murr, S. M. Gaytan, D. A. Ramirez, E. Martinez, J. Hernandez, K. N. Amato, P. W. Shindo, F. R. Medina, R. B. Wicker, Metal fabrication by additive manufacturing using laser and

electron beam melting technologies, *Journal of Materials Science & Technology* **28** (2012) 42-54. https://doi.org/10.1016/S2238-7854(12)70009-1

[3] W. E. Frazier, Metal additive manufacturing: a review, *Journal of Materials Engineering and Performance* **23** (2014) 1917-1928. https://doi.org/10.1007/s11665-014-0958-z

[4] D. Herzog, V. Seyda, E. Wycisk, C. Emmelmann, Additive manufacturing of metals, *Acta Materialia* **117** (2016) 371-392. https://doi.org/10.1016/j.actamat.2016.07.019

[5] C. Körner, Additive manufacturing of metallic components by selective electron beam melting, *International Materials Reviews* **61** (2016) 361-377. https://doi.org/10.1080/09506608.2016.1176289

[6] T.M. Braun, D.T. Schwartz. The emerging role of electrodeposition in additive manufacturing. *The Electrochemical Society Interface* **25** (2016) 69-73. https://doi.org/10.1149/2.F07161if

[7] X. Li, P. Ming, S. Ao, W. Wang, Review of additive electrochemical micro-manufacturing technology, *International Journal of Machine Tools and Manufacture* **173** (2022) 103848. https://doi.org/10.1016/j.ijmachtools.2021.103848

[8] G. Ercolano, T. Zambelli, C. van Nisselroy, D. Momotenko, J. Vörös, T. Merle, W.W. Koelmans Multiscale additive manufacturing of metal microstructures, *Advanced Engineering Materials* **22** (2020) 1900961. https://doi.org/10.1002/adem.201900961

[9] L. Hirt, R.R. Grüter, T. Berthelot, R. Cornut, J. Vörös, T. Zambelli, Local surface modification via confined electrochemical deposition with FluidFM, *RSC Advances* **103** (2015) 84517-84522. https://doi.org/10.1039/c5ra07239e

[10] W. Ren, J. Xu, Z. Lian, P. Yu, H. Yu, Modeling and experimental study of the localized electrochemical micro additive manufacturing technology based on the fluidFM. *Materials* **13** (2020) 2783. https://doi.org/10.3390/ma13122783

[11] G. Ercolano, C. van Nisselroy, T. Merle, J. Vörös, D. Momotenko, W. W. Koelmans, T. Zambelli Additive manufacturing of sub-micron to sub-mm metal structures with hollow AFM cantilevers, *Micromachines* **11** (2020) 6. https://doi.org/10.3390/mi11010006

[12] W. Ren, J. Xu, Z. Lian, X. Sun, Z. Xu, H. Yu, Localized electrodeposition micro additive manufacturing of pure copper microstructures, *International Journal of Extreme Manufacturing* **4** (2021) 015101. https://doi.org/10.1088/2631-7990/ac3963

[13] A. Ambrosi, R. D. Webster, M. Pumera, Electrochemically driven multi-material 3D-printing. *Applied Materials Today* **18** (2020) 100530. https://doi.org/10.1016/j.apmt.2019.100530

[14] S. Burlison, M. Minary-Jolandan, Multiphysics simulation of microscale copper printing by confined electrodeposition using a nozzle array, *Journal of Applied Physics* **131** (2022) 055303. https://doi.org/10.1063/5.0072183

[15] Y. Guo, P. Liu, P. Jiang, Y. Hua, K. Shi, H. Zheng, Y. Yang, A flow-rate-controlled double-nozzles approach for electrochemical additive manufacturing. *Virtual and Physical Prototyping* **17** (2022) 52-68. https://doi.org/10.1080/17452759.2021.1989751

[16] X. Chen, X. Liu, P. Childs, N. Brandon, B. Wu, A low cost desktop electrochemical metal 3D printer, *Advanced Materials Technologies* **10** (2017) 1700148. https://doi.org/10.1002/admt.201700148

[17] F. Zhang, D. Li, W. Rong, L. Yang, Y. Zhang, Study of microscale meniscus confined electrodeposition based on COMSOL, *Micromachines* **12** (2021) 1591. https://doi.org/10.3390/mi12121591

[18] X. Chen, X. Liu, M. Ouyang, J. Chen, O. Taiwo, Y. Xia, P. Childs, N.P. Brandon, B. Wu, Multi-metal 4D printing with a desktop electrochemical 3D printer, *Scientific Reports* **9** (2019) 3973. https://doi.org/10.1038/s41598-019-40774-5

[19] A. Kamaraj, S. Lewis, M. Sundaram, Numerical study of localized electrochemical deposition for micro electrochemical additive manufacturing, *Procedia CIRP* **42** (2016) 788-792. https://doi.org/10.1016/j.procir.2016.02.320

[20] V. M. Volgin, V. V. Lyubimov, I. V. Gnidina, A. D. Davydov, T. B. Kabanova, Simulation of localized electrodeposition of microwires and microtubes, *Procedia CIRP* **68** (2018) 242-247. https://doi.org/10.1016/j.procir.2017.12.056
[21] E. M. El-Giar, R. A. Said, G. E. Bridges, D. J. Thomson, Localized electrochemical deposition of copper microstructures, *Journal of The Electrochemical Society* **147** (2000) 586-591. https://doi.org/10.1149/1.1393237
[22] C. Y. Lee, C. S. Lin, B. R. Lin, Localized electrochemical deposition process improvement by using different anodes and deposition directions, *Journal of Micromechanics and Microengineering* **18** (2008) 105008. https://doi.org/10.1088/0960-1317/18/10/105008
[23] J. C. Lin, T. K. Chang, J. H. Yang, Y. S. Chen, C. L. Chuang, Localized electrochemical deposition of micrometer copper columns by pulse plating, *Electrochimica Acta* **55** (2010) 1888-1894. https://doi.org/10.1016/j.electacta.2009.11.002
[24] M. M. Sundaram, A. B. Kamaraj, V. S. Kumar, Mask-less electrochemical additive manufacturing: a feasibility study, *Journal of Manufacturing Science and Engineering* **137** (2015) 021006. https://doi.org/10.1115/1.4029022
[25] M. Sundaram, A. B. Kamaraj, G. Lillie, Experimental study of localized electrochemical deposition of Ni-Cu alloy using a moving anode, *Procedia CIRP* **68** (2018) 227-231. https://doi.org/10.1016/j.procir.2017.12.053
[26] G. Vasyliev, V. Vorobyova, D. Uschapovskiy, O. Linyucheva, Local electrochemical deposition of copper from sulfate solution, *Journal of Electrochemical Science and Engineering* **12** (2022) 557-563. http://dx.doi.org/10.5599/jese.1352
[27] L.T. Romankiw, A path: from electroplating through lithographic masks in electronics to LIGA in MEMS, *Electrochimica Acta* **42** (1997) 2985-3005. https://doi.org/10.1016/S0013-4686(97)00146-1
[28] H. Hu, H.J. Kim, S. Somnath, Tip-based nanofabrication for scalable manufacturing, *Micromachines* **8** (2017) 90–120. https://doi.org/10.3390/mi8030090
[29] L. Ménager, M. Soueidan, B. Allard, V. Bley, B. Schlegel, A -Scale Alternative Interconnection Solution of Semiconductor Dice Compatible with Power Modules 3-D Integration, *IEEE Transactions on Power Electronics* **25** (2010) 1667-1670. https://doi.org/10.1109/TPEL.2010.2041557
[30] Electrode Growth Next to an Insulator, [Online]. Available: https://www.comsol.com/model/electrode-growth-next-to-an-insulator-10212
[31] K. Bouzek, K. Borve, O.A. Lorentsen, K. Osmundsen, I. Rousar, J. Thonstad, Current Distribution at the Electrodes in Zinc Electrowinning Cells, *Journal of The Electrochemical Society* **142** (1995) 64–69**.** https://doi.org/10.1149/1.2043939
[32] L. I. Kadaner, *Dovidnyk po hal'vanostehiyi*, Tekhnika, Kyiv, USSR, 1976, p. 253.
[33] X. Feng l, H. Cao, H. Yu, L. Gaol, M. Lil. Study of internal stress on electroplating copper used in through silicon via filling, 12*th International Conference on Electronic Packaging Technology & High Density Packaging*, Shanghai, China, 2011, p.1-4. http://dx.doi.org/10.1109/ICEPT.2011.6067001
[34] R. Winand, Electrocrystallization-theory and applications, *Hydrometallurgy* **29** (1992) 567-598. https://doi.org/10.1016/0304-386X(92)90033-V